Indian J Phys (April 2012) 86(4):267–272
DOI 10.1007/s12648-012-0051-0

ORIGINAL PAPER

Fabrication of CdMnTe semiconductor as radiation detector

L A Najam[1]*, N Y Jamil[1] and R M Yousif[2]

[1]Department of Physics, College of Science, Mosul University, Mosul, Nineveh 00964, Iraq

[2]Department of Environmental Science Technology, College of Environmental Science and Technology, Mosul University, Mosul, Ninevah 00964, Iraq

Received: 18 July 2010 / Accepted: 27 February 2011 / Published online: 11 May 2012

Abstract: In this work, devices have been fabricated as to be nuclear detector, from p-CdMnTe. Three devices were prepared: First planar detector with (Au) ohmic contact on both sides**;** Second as schottky type device of In-CdMnTe with (Au) ohmic contact on the back face; and thirdly metal oxide semiconductor (MOS) device for which the samples annealed under Oxygen flow for (2 h.) at 700 °C, this device (MOS) when connected to conventional nuclear spectroscopy gave reasonable but not high quality signals due to irradiating with ^{137}Cs, ^{241}Am and (^{137}Cs + ^{241}Am). Matlab- software based on numerical methods is used to analyze the data. Resolution through the Full Width at Half Maximum and the area under the peak and the error for this detector are presented.

Keywords: CdMnTe; Gamma ray detector; II–VI materials; MOS device; Energy resolution

PACS No.: 29.40.Wk

1. Introduction

There are increasing demands for new semiconductor detectors capable of detecting hard X-ray and gamma rays. For imaging devices, their good energy resolution and the ability to fabricate compact arrays are very attractive features in comparison to the inorganic scintillation detectors coupled to either photodiodes or photomultipliers tubes [1].

The fast developments in compound semiconductor detectors are reviewed, high lighting the last spectroscopic performance from devices fabricated from a range of wide bandgap materials [2].

Cadmium zinc telluride (CZT) is one of the most promising materials for the production of large-volume gamma-ray spectrometers and imaging arrays operable at room temperature. However, because of deficiencies in the quality of the material, commercial high-resolution CZT spectrometers are still limited to relatively small dimensions [3] where, vanadium doped $Cd_{1-x}Mn_xTe$ crystals with high resistivity $>10^{10}$ Ωcm fabricated as gamma-ray detector with $x = 0.15$ and 0.45 as planar type to show general separation of gamma-ray (59.5 keV) line from lower X-ray line [4]. Many techniques are being used in order to Synthesize nano-micro materials falling under the realm of nanotechnology [5].

Solid state nuclear track detector (SSNTD) based systems being the best suited for large scale passive monitoring [6].

An attempt has been made to explore the possibility of using SSNTDs for the estimation of gamma and neutron doses [7].

Mycielski et al. [8] found that the composition homogeneity of the large single crystals of the ternary compound seems to be easier to achieve the case of (Cd, Mn, Te) because the segregation coefficient of Mn in CdTe is negligible with respect to that (approximately 1.3) of Zn. Only 15 % of MnTe has to be added to CdTe to reach the best for the detector application value of the energy gap in the range (1.7–2.2 eV), while the necessary amount of ZnTe is over 30 %.

Comparing of CdMnTe with CdZnTe it shows that the growth of high quality CdMnTe crystals is easier due to the lack of segregation of Mn in CdTe and obtaining the optimum value of energy gap is easier due to its much stronger composition [9, 10].

Cadmium manganese telluride ($Cd_{1-x}Mn_xTe$) is a diluted magnetic semiconductor known to forms a ternary alloy

*Corresponding author, E-mail: dr_laithahmed@yahoo.com

Fig. 1 CdMnTe material

of zinc blended structure with ($0 < x < 0.77$) which forms the basis for many important devices such as IR detectors, solar cells, magnetic sensors, optical isolators, and visible and near IR laser [11, 12].

In this work CdMnTe will be used as nuclear detector in three form devices.

2. Experimental details

Samples of *p*-CdMnTe used in this study were grown by high pressure Bridgman method, with sizes 5 mm diameter and 1 mm thickness. The crystals were polished mechanically and then polished with alumina suspension. This is followed by Br/methanol chemical etching before the metal contacting, the crystals were rinsed in a gradually diluted solution, followed by final rinse in pure methanol. Finally, the crystals were quickly blown dry by using acetone (more information see) [13].

p-CdMnTe has resistivity of $\sim 10^4\ \Omega$ cm as grown material Fig. 1. The samples of CdMnTe were annealed under vacuum at (700 ± 3 °C) for a period of (2 and 5 h). This caused a change in the resistivity to about (10^7) Ω cm. Ohmic contacts to the prepared samples Au-CdMnTe-Au were done by vacuum thermal evaporation. The contact was then annealed at a temperature of 250 °C for 15 min for all samples.

Samples were prepared in one of the following types:

(1) Planar type detector.
(2) Schottky type detector.
(3) MOS device detector.

The planar type detector crystals are annealed at 700 °C, treated with quick mechanically polishing and chemical etching. This gives the samples mirror finished surfaces.

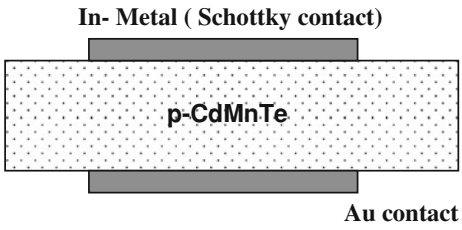

Fig. 2 Schottky type detector sample

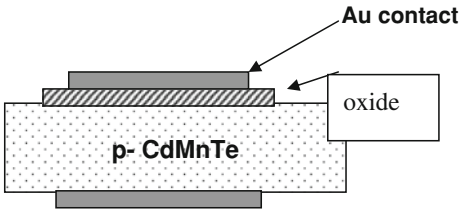

Fig. 3 MOS device sample

The gold electrode was evaporated (~2,000 Å thickness) on the both sides.

Schottky type detector (Fig. 2), formed by evaporating (In) electrode on one top face of CdMnTe sample, and ohmic contact of Au formed on the opposite face of the sample was formed.

For third type of samples annealed under oxygen flow for 2 h at 700 °C, CdO thin film expected to be formed this gives MOS structure. Back face of the samples are polished. Again using the vacuum system, for Au-contact is evaporated on both faces and annealed to 250 °C for 15 min (for the back face only) as in Fig. 3.

3. Results and discussions

3.1. Testing the detector

Two types of test were employed:

1. Oscilloscope pulse test

The circuit in Fig. 4 is used to perform a priliminary test on the samples. In spite of the fact that our oscilloscope can not store a particular pulse, large number of pulses were seen on the screen. The augmentation in the intensity of pulses was noticed when the radioactive source was brought near to the detector. However there remain some smaller pulses even when the radioactive source was removed. These pulses correspond to background noise.

2. Multi channel analyzer (MCA) test

The same circuit mentioned above is used to carry out the actual testing of the detector. The Oscilloscope is replaced by the input of Spectroscopy amplifier. The output of the spectroscopy amplifier is fed to the MCA (4,095

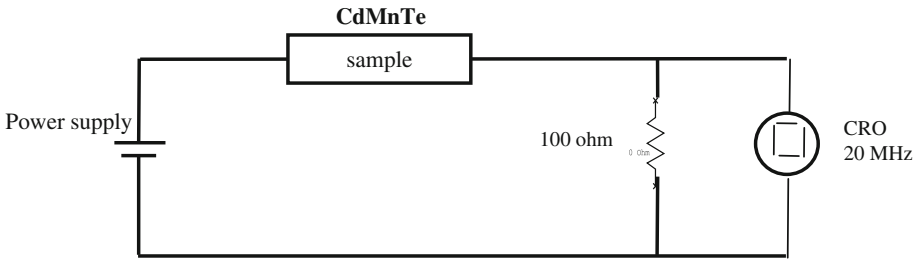

Fig. 4 Circuit used for pulse test

Channel), pulse height, is carried out for the following cases:

1. When a radioactive source ^{137}Cs of activity (1.06 μCi) is brought near the detector, the spectrum for this test is shown in Fig. 5(a). Figure 5(b) is the same as in Fig. 5(a) expect the time was longer.
2. When a radioactive source ^{241}Am of activity (5.0 μCi) is brought near the detector, the spectrum for this test is shown in Fig. 6(a). The spectrum displayed in Fig. 6(b) is the same as that in Fig. 6(a) except the fact that the time is longer.
3. When both the sources ^{137}Cs and ^{241}Am were brought near the detector, the spectrum for this test is shown in Fig. 7.

In order to reach high resistivity the crystal post grown annealed in addition of forming of the oxide layer. The high resistivity is always desired in order to achieve low electronic noise, in addition to the best performance.

In order to give some features of the CdMnTe detector in this work, it is necessary to present information concerning the resolving power through full width at half

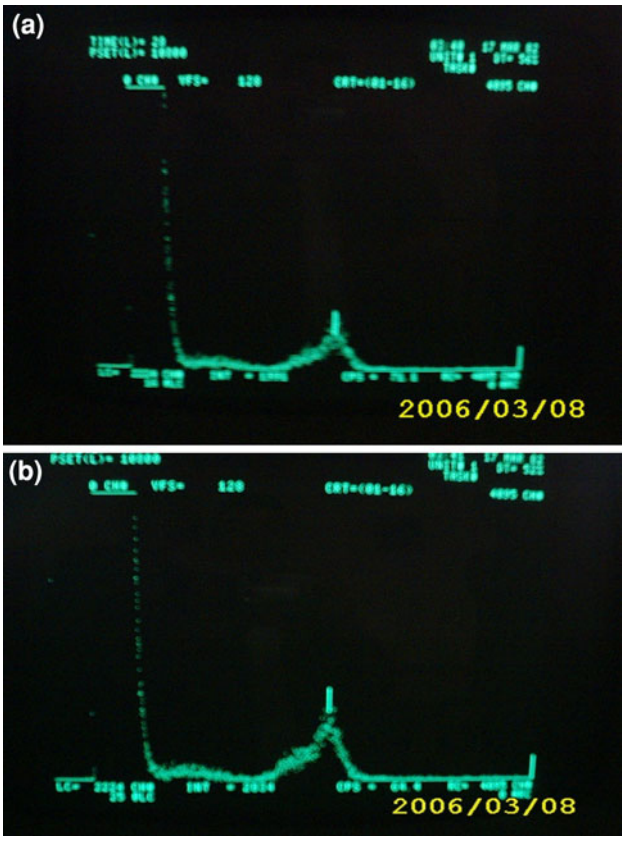

Fig. 5 (**a**) The observed figure for the radioactive source ^{137}Cs brought near the sample ($t = 59$ s). (**b**) The observed figure obtained due to irradiating the sample with ^{137}Cs with long time ($t = 120$ s)

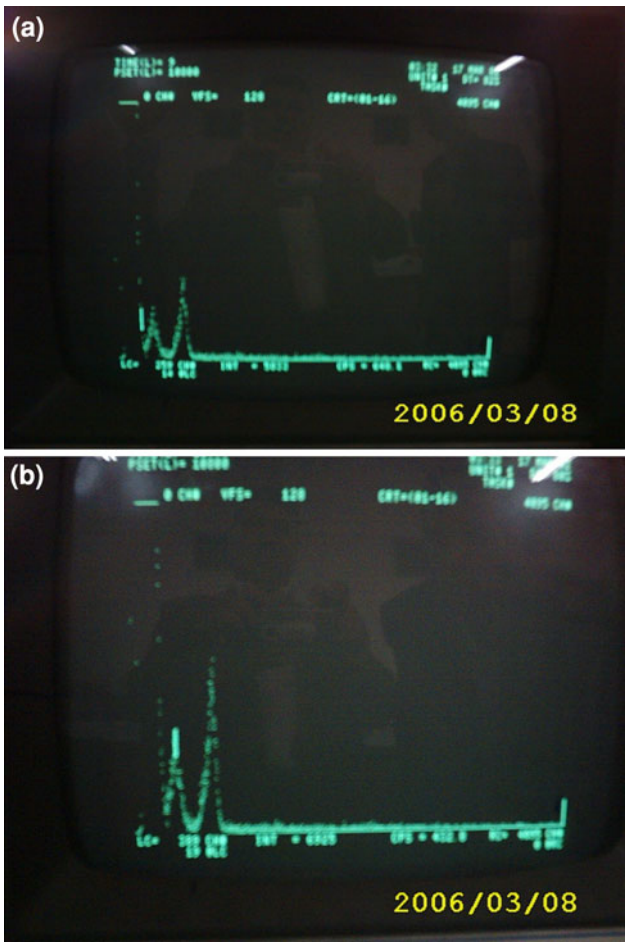

Fig. 6 (**a**) The observed figure obtained due to irradiating the sample with ^{241}Am. (**b**) The observed figure obtained due to irradiating the sample with ^{241}Am with longer time

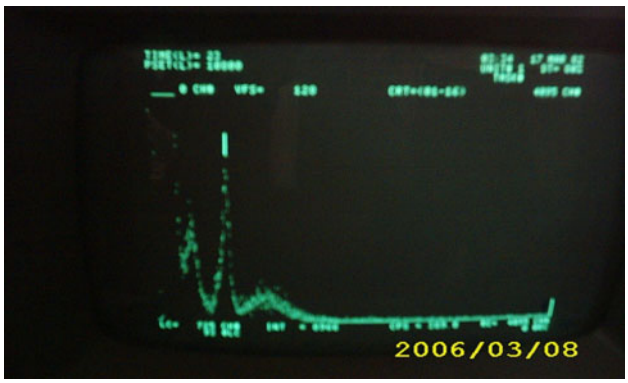

Fig. 7 The observed figure for the radioactive sources ^{137}Cs and ^{241}Am brought near the sample

maximum (FWHM), area under the peak and error calculations for this type of detector. Due to the fact that we can not obtain direct numerical data from our MCA, to carry out such analysis and also to the relatively poor stability of our detector, a modified data analysis technique is used to get the above information.

The following steps are taken to calculate (FWHM) area under the curve and error with acceptable accuracy:

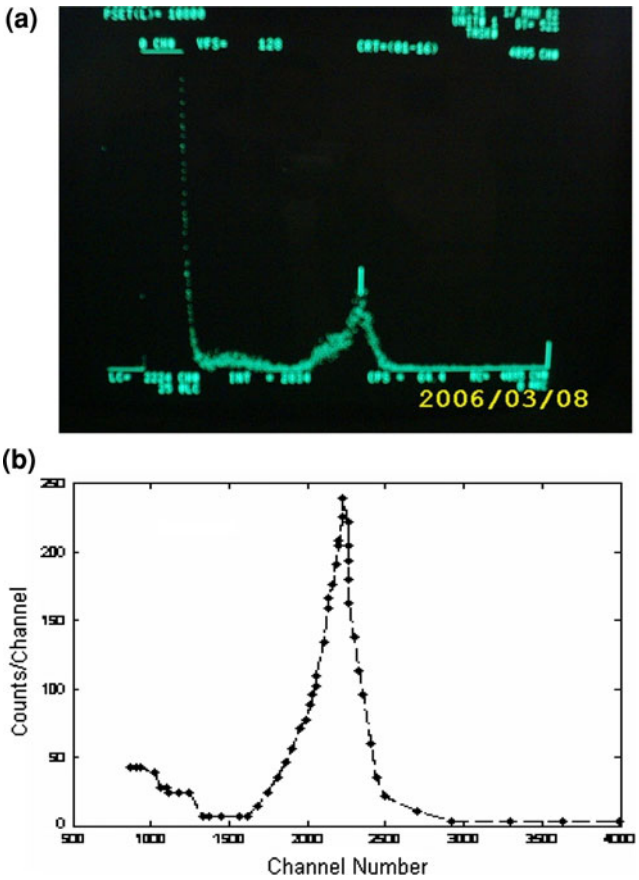

Fig. 8 (**a**) Repeating of Fig. 5(b). (**b**) The reproduced figure of Fig. 8(a)

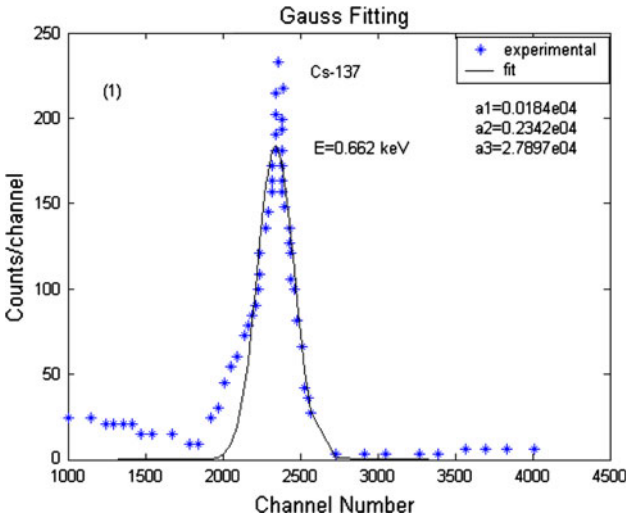

Fig. 9 The fitted peak of Fig. 5(a)

1. Digital pictures are taken for the spectra appearing on the MCA screen.
2. Numerical data are extracted from the pictures using a mathlab based program called Convert [14]. This program can rebuild numerical data in x–y coordinates from any curve or plot on a digital jpg or TIFF or many other format pictures. Any number of data points can be selected according to the user specification. Each picture was analyzed using the program and plots are reproduced. The reproduced plots are almost exact replica of the original figure in the pictures. Here, however, we have the numerical data of the figure in the addition to the plots. Examples of results can be seen in Fig. 8(a), (b).
3. Numerical data obtained in step 2 are fitted with gaussian type curve of the form:

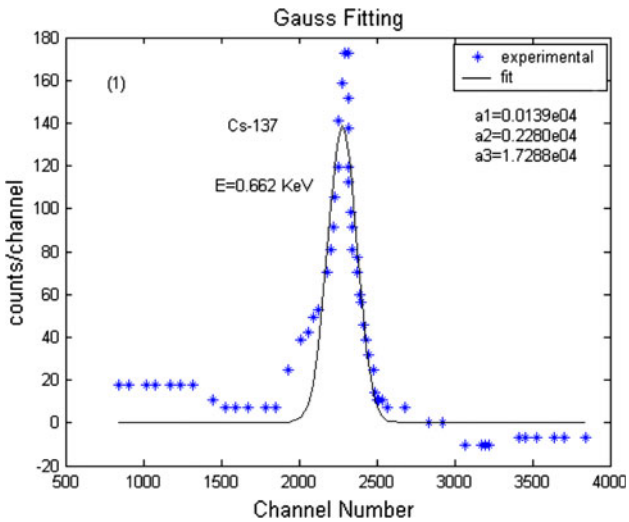

Fig. 10 The fitted peak Fig. 5(b)

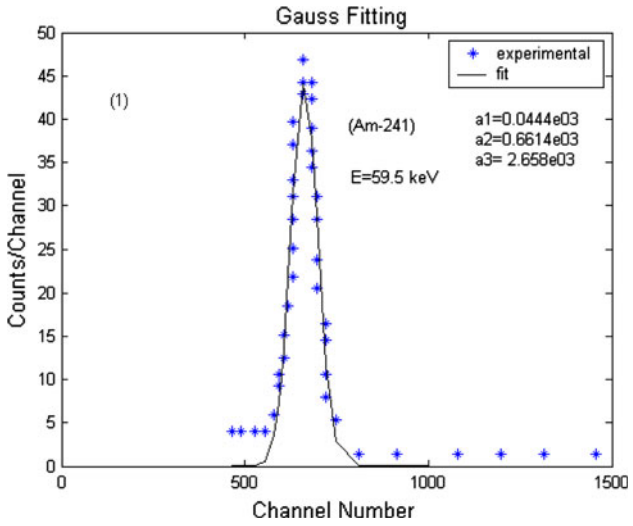

Fig. 11 The fitted peak of Fig. 6(a)

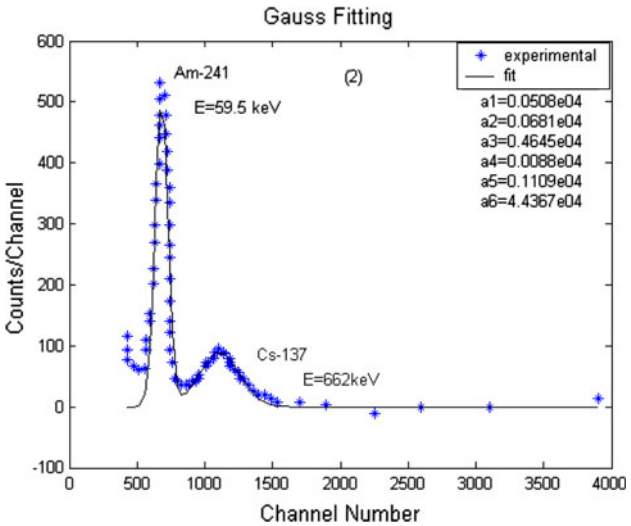

Fig. 13 The fitted peaks of Fig. 7

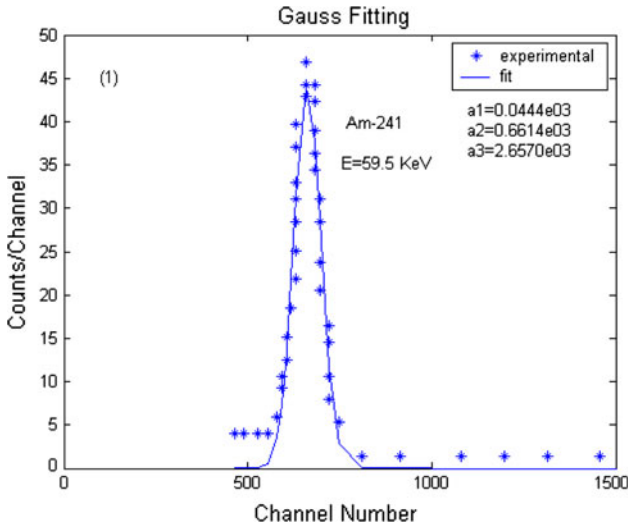

Fig. 12 The fitted peak of Fig. 6(b)

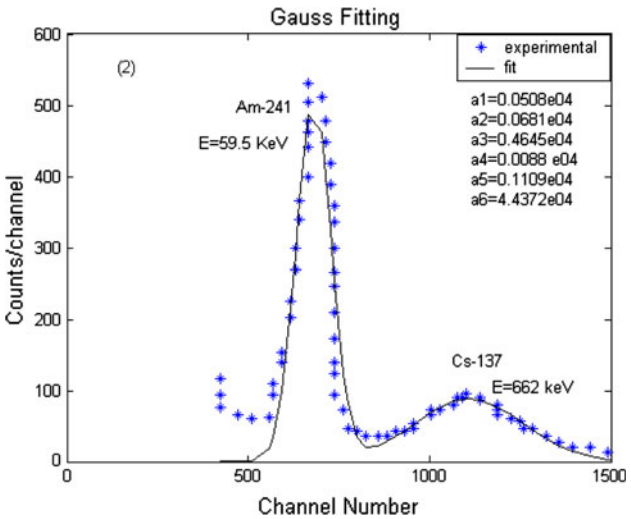

Fig. 14 The fitted peaks of Fig. 7 with different channel number

$$\text{Count} \cdot \text{No.} = a_1 e^{-(E-a_2)^2/a_3} \quad (1)$$

where a_1, a_2 and a_3 are fitting parameters representing the peak counts average energy and (Standard deviation)^2 respectively. For Figure that has two peaks a double gausian fit of the following form is used:

$$\text{Count} \cdot \text{No.} = a_1 e^{-(E-a_2)^2/a_3} + a_4 e^{-(E-a_5)^2/a_6} \quad (2)$$

a_4, a_5, a_6 are similar to a_1, a_2, a_3 but for the second peak. Hence the parameters determined the shape of the peak. Figures 9–14 show the results of actual data and fitted curves obtained for irradiating the sample with the radioactive sources ^{137}Cs, ^{241}Am and (^{137}Cs + ^{241}Am).

4. Once the empirical formula, describing the peak, is known, it is fairy straight forward to evaluate (FWHM) and area under the curve and errors.The resolution is defined as:

$$R = \Delta E/E = (\text{FWHM})/E$$

where ΔE is the peak width at half maximum. Mathlab has a useful facility much similar to that of the cursor in an MCA, it can activitated by a ginput command, three data points using this command are registed for the peak count number, and the sides count number.

As far as evaluating the area under the peak is concerned, this area is evaluated using the mathematical equation:

$$A = \int f(E)\, dE \quad (3)$$

Table 1 The information's included peak channel, FWHM, resolution, area under peak and error

Figure number	Peak number	Peak channel (Ch.)	FWHM (Ch.)	Resolution (%)	Area under peak	Error (%)
5a (9)	1	2,302	169	7.3	3.23×10^4	15.15
5b [10]	1	2,358	217	9.2	5.43×10^4	13.30
6a [11]	1	658	83	12.6	3.44×10^3	3.72
6b [12]	1	658	85	12.9	4.05×10^3	5.08
7 [13]	2	668	119	17.8	5.95×10^4	48.61
		1,101	171	15.5	2.48	14.30
7 [14]	2	668	120	17.96	6.09×10^4	41.83
7 [14] with different channel number	2	1,101	171	15.5	0.237	23.73

where f(E) is the energy distribution function as obtained from the MCA, E is the energy proportional to the channel number.

Having obtained f(E) from Eq. 3, with the known free parameters, trapezoidal rule integration is performed to obtain the area under the peak for each case in much similar way to that performed by the MCA.

For calculating the errors associated with this type of procedure, again here we copy techniques employed by the MCA by defining the error as:

$$\text{Error} = \left(y - a_1 e^{-(E-a_2)^2/a_3}\right) \tag{4}$$

where y is the actual count number.

Again here the mathlab program is used to calculate the errors. The results are shown in Table 1.

4. Conclusions

Three devices were prepared from *p*-CdMnTe as planar detector, Schottky device, and MOS device. The last one when connected to conventional nuclear spectroscopy gave reasonable but not high quality signals due to irradiating with ^{137}Cs, ^{241}Am and (^{137}Cs + ^{241}Am). For which we think that the expected oxide layer on the sample surface was the reason to get that detected signal.

References

[1] T Takahashi and S Watanabe *IEEE Trans. Nucl. Sci.* **48** 950 (2001)
[2] P J Sellin *Nucl. Instrum. Methods* **A513** 332 (2003)
[3] G A Carini, A E Bolotnikov, G S Camarda and R B James *Nucl. Instrum. Methods* **A579** 120 (2007)
[4] A Burger, K Chattopadhyay, H Chen, J N dap Olivier, M Triredi Xiaoy, W Kuteher Susan, R Chen and D Robert *J. Cryst. Growth* **198/199** 872 (1999)
[5] S Mitra, A Mandal, S Banerjee, A, Datta, S Bhattacharya, A Bose and D Chakravorty *Indian J. Phys.* **85** 649 (2011)
[6] P Dash, P Mallick, H Rath, B N Dash, A Tripathi, J Prakash, D K Avasthi, P V Satyam and N C Mishra *Indian J. Phys.* **84** 1391 (2010)
[7] M C Santosh Kumar and B Pradeep *Indian J. Phys.* **85** 401 (2011)
[8] A Mycielski, A Burger, M Sowinska, M Groza, A P Wojnar, B Witkowska, W Kaliszek and P Siffert *Phys. Status Solidi*, **2** 1578 (2005)
[9] M Witkowska-Bran, A Mycielski, D Kochanows, A J Szadlkowski and R B James *Nucl. Sci. Sympo. Conf. Rec. IEEE* 327 (2008).
[10] K H Kim, V Carcelen, A E Bolotnikov, G S Camarda, R Gul, A Hossain, G Yang, Y G Cui and R B James *J. Electron. Mater.* **39** 1015 (2010)
[11] K H Kim, A E Bolotnikov, G S Camarda, A Hossain, R Gul, G Yang, Y G Cui, J Prochazka, J Franc, J Hong and R B James *J. Appl. Phys.* **109** 113715 (2011)
[12] K H Kim, H Cho Shin, H Suh Jong, J Hong and U Kim Sun *IEEE Trans. Nucl. Sci.* **56** 858 (2009)
[13] L A Najam PhD Thesis (University of Mosul, College of Science, Physics Department, Iraq) (2006)
[14] A A Azooz *Instrum. Exp. Tech.* **54** 364 (2011)